

Article

# Study of the AMP-activated Protein Kinase Role in Energy Metabolism Changes during the Postmortem Aging of Yak *Longissimus dorsal*

Yayuan Yang <sup>1</sup>, Ling Han <sup>1,\*</sup>, Qunli Yu <sup>1</sup>, Yongfang Gao <sup>1</sup> and Rende Song <sup>2</sup>

<sup>1</sup> College of Food Science and Engineering, Gansu Agricultural University, Lanzhou, Gansu 730070, China; yancyangzxl@163.com (Y.Y.); yuqunlisci@163.com (Q.Y.); gyfgyfgyf123ying@163.com (Y.G.)

<sup>2</sup> Qinghai Animal and Veterinary Sciences Work Station, No. 189, Xinjian road, Yushu prefecture, Qinghai 815000, China; xiaoyuan520@aliyun.com

\* Correspondence: hlsciggyx@126.com; Tel./Fax: +1 86-0931-7631201

Received: 3 February 2020; Accepted: 2 March 2020; Published: 4 March 2020



**Simple Summary:** Pale, soft, and exudative (PSE) meat is characterized by a pallid, sodden, and spongy appearance. Studies show that an early buildup of lactic acid due to rapid postmortem glycolysis, coupled with high muscle temperature, is the cause of PSE meat, although the precise molecular mechanisms remain poorly defined. We hypothesized that adenosine monophosphate activated protein kinase (AMPK) is the key factor regulating postmortem glycolysis in meat. To this end, we respectively activated and inhibited AMPK in yak muscle using AICAR and STO-609 and analyzed the metabolism parameters. The objective of this study was to establish the crucial role of AMPK in postmortem glycolysis and the possibility of targeting AMPK in order to reduce glycolysis and minimize the risk of PSE meat. Yaks are adapted to higher altitudes and lower atmospheric oxygen levels. Therefore, the activity of the yak AMPK is increased under hypoxic adaptation, which accelerates glycolysis and optimizes energy production. We further investigated the role of AMPK in the regulation of postmortem muscle glycolysis using the AMPK inhibitor STO-609 and specific activator AICAR. The objective of this study was to confirm the crucial role of AMPK in postmortem glycolysis and its potential as a target to reduce glycolysis and study of energy metabolism in yak.

**Abstract:** To explore the postmortem physiological mechanism of muscle, activity of adenosine monophosphate activated protein kinase (AMPK) as well as its role in energy metabolism of postmortem yaks were studied. In this experiment, we injected 5-amino-1-beta-d-furanonyl imidazole-4-formamide (AICAR), a specific activator of AMPK, and STO-609 to observe the changes in glycolysis, energy metabolism, AMPK activity, and AMPK gene expression (PRKA1 and PRKA2) in postmortem yaks during maturation. The results showed that AICAR could increase the expression of the PRKKA1 and PRKAA2 genes, activate AMPK and increase its activity. The effects of AICAR include a lower concentration of ATP, an increase in AMP production, an acceleration of glycolysis, an increase in the lactic acid concentration, and a decrease in the pH value. In contrast, STO-609 had the opposite effect. Under hypoxic adaptation, the activity of the meat AMPK increased, which accelerated glycolysis and metabolism and more effectively regulated energy metabolism. Therefore, this study lays the foundation for establishing a theoretical system of energy metabolism in postmortem yak meat.

**Keywords:** AICAR; STO-609; AMP-activated protein kinase; energy metabolism; skeletal muscle

## 1. Introduction

Yaks adapted to high altitudes because of the colder climate. This process included the maintenance of the production of adenosine triphosphate (ATP) through an increase in glycolysis. Studies have shown that yaks have specific metabolic mechanisms that enable them to adapt to a hypoxic environment to attain an adequate supply of energy and a demand balance under hypoxic conditions [1–3]. AMP-activated protein kinase (AMPK), as an important cellular energy sensor, is critical for the regulation of the metabolism of energy and the subsequent quality of the meat. Under hypoxic conditions, the body is under stress, metabolism is strengthened, ATP consumption is increased, the ATP concentration is decreased, the AMP production is increased, and a high concentration of 5'-AMP and AMPK gamma subunits interact to activate AMPK. Ding et al. studied the activity of lactate dehydrogenase (LDH) in yaks at three different altitudes, and its activity positively correlated with altitude [4]. LDH is the key enzyme for anaerobic glycolysis, indicating that yaks at higher altitudes are more dependent on energy metabolism [5–8].

The enzyme AMPK is a heterotrimer consisting of  $\alpha$ ,  $\beta$ , and  $\gamma$  subunits. Its primary role is thought to be the critical regulation of energy metabolism [9–12]. AMP/ATP ratio increase in muscle cells is thought to result in the activation of AMPK. This activation results in the phosphorylation of AMPK at Thr172 by a kinase that remains unidentified. Following its activation, AMPK activates glycogenolysis/glycolysis and consuming/catabolic pathways that generate ATP [2,13–16]. Thus, the data accumulated confirms that hypoxia is a characteristic of postmortem skeletal muscle.

Previous research demonstrated the activation of AMPK in pork loins which develop into PSE meat. This finding suggests that a key role of AMPK is regulation of postmortem glycolysis [17]. Therefore, the role of AMPK may be the regulation of glycolysis in postmortem skeletal muscle. If so, the enzyme may be a logical target to manipulate to intervene in the process of PSE development and cause its reduction, since AMPK activity depends on the postmortem skeletal muscle pH values. Therefore, we further studied AMPK's role in muscle glycolysis regulation in postmortem meat, using specific AMPK activators and inhibitors to detect whether the induction of AMPK by 5-amino-1- $\beta$ -D-ribofuranosyl-imidazole-4-carboxamide (AICAR) and STO-609 affect postmortem muscle glycolysis. Recent research in rat skeletal muscle used a cell-permeable compound AICAR to activate AMPK to study its possible role in controlling glucose metabolism in this tissue [18]. These studies involved administration of either in vivo or in vitro AICAR to skeletal muscle for varying amounts of time. In addition, different methods were used to evaluate the changes of carbohydrate metabolism. These methods included a muscle preparation that had been isolated and incubated, a hindquarter preparation that had been perfused, or tissues analyses following a euglycemic clamp or treatment. To our knowledge, the effect of reactive AICAR on the AMP-activated protein kinase of mice longissimus lumborum has only been examined in one study. Among other studies, we found that injecting a dose of 250 mg/kg AICAR had no effect on the glycogen binding in the diaphragm (respiratory muscle) of mice fed or fasting [19]. At the same time, the effects on glucose transport in yak skeletal muscle due to AICAR treatment remain unclear. In comparison, the inhibitory effect of STO-609, an AMPK inhibitor, was used to inhibit food intake and therefore weight gain in mammals [20].

This study was performed to analyze the effects of AICAR and STO-609 on pH, lactic acid, energy metabolism, AMPK activity, and AMPK mRNA (PRKAA1, PRKAA2) expression in postmortem yak muscle. It lays the foundation for establishing a theoretical system of energy metabolism in postmortem yak meat.

## 2. Materials and Methods

### 2.1. Animal Treatment

The longissimus dorsal (LD) is the 12th rib that is anterior to the last lumbar vertebrae, and they were randomly extracted from a slaughterhouse (Yushu Tibetan Autonomous Prefecture, Qinghai Province, China). Animals used in the experiment process is to follow the national slaughter and

processing Standardization Technical Committee (SAC / TC516). Ten Qinghai yak bulls that were the same age (36–38 months old) and weighed 241–280 kg were fed the same diet from the same batch. Each yak was tested. The ribs were immediately frozen in liquid nitrogen as the sample for 0 h. The remaining amount of each 40 g aliquot of the muscle pieces was divided into two portions. One portion was treated as the control, while the other was treated with injections of a 1:1 ratio (w/v) of 10 mM AICAR (Sigma A9978) and STO-609 (Sigma Aldrich). All samples were subsequently stored at 4 °C for 12, 24, 72, 120, and 168 h. All samples collected at these times were stored at –80 °C until further use.

## 2.2. Measurement of the pH

The pH values of all the loins at each time point were measured using a Testo®230 meter (Testo GmbH & Co., Lenzkirch, Germany). pH values were measured using pH meter calibrated standard buffer solutions with pH values equal to 4.0 and 7.0 (Mallinckrodt Chemicals, Phillipsburg, NJ, USA). Prior to calibration, buffers solutions were stored at 20 °C according to a procedure mentioned elsewhere [21].

## 2.3. Lactic Acid Concentration

A total of 500 mg of frozen muscle samples was homogenized using 500 mL of 0.9% saline and then centrifuged at 4200 g at 4 °C for 10 min. Following a 50-fold dilution of the supernatant, standard commercial kits from Blue Gene Biotech Co. (Shanghai, China) were used to measure the lactic acid contents. The optical density (OD450) was measured immediately using an ELISA microplate reader. The values measured at each concentration of the standard were used to prepare a calibration curve [22].

## 2.4. ATP, ADP, AMP, and IMP Activity

As previously described by Hou's method, approximately 3 g of frozen muscle was centrifuged for 10 min at 15,000 × g (Heraeus, Biofuge fresco, Hanau, Germany) at 4 °C. The supernatant was mixed with 1.44 mL of 0.85 M K<sub>2</sub>CO<sub>3</sub> and filtered through a 0.2 µm membrane. The content of ATP, ADP, AMP, and IMP was analyzed using Agilent 1100 Chromatography at 254 nm detection wavelength. A reversed phase C18 column was used, and the flow rate was 1 mL/min. Quantitative analysis was conducted on the basis of retention time and peak area [23].

## 2.5. AMPK Activity

AMPK activity measurements were based on AMPK-specific phosphorylation of a SAMS peptide [22]. Briefly, SAMS peptide substrate (His-Met-Arg-Ser-Ala-Met-Ser-Gly-Leu-His-Leu-Val-Lys-Arg-Arg, obtained from Invitrogen, Carlsbad, CA, USA) was used for the assay. As-obtained muscle homogenate was centrifuged at 1,300g at 4 °C for 5 min. Ten microlitres of supernatant was incubated for 10 min at 37 °C at pH 7.0. Its final volume was 50 µL, and it contained 0.2 mM of ATP + 2 µCi [32P] ATP, 0.2 of mM AMP, 5 mM of MgCl<sub>2</sub>, 0.2 of mM SAMS peptide, 80 of mM NaCl, 0.8 mM of dithiothreitol, 0.8 mM of EDTA, 8% (w/v) of glycerol, and 40 mM of 4-2-hydroxyethyl-1-piperazineethanesulfonic acid. Twenty microliters of this mixtures was removed and placed on Whatman P81 filter paper (Whatman, Maidstone, UK) that had been cut into 2 cm × 2 cm pieces. Six washes of 1% phosphoric acid were conducted to remove the ATP. Finally, the filter paper was immersed in 3 mL of Scinti Verse (obtained from Fisher Scientific, Waltham, MA, USA). AMPK nanomolar peptide activity phosphorylation was expressed per minute per gram of muscle.

## 2.6. Immunoblotting

AMPK was analyzed using the frozen yak LD muscle derived from these methods as previously described [24]. Briefly, 0.05 g of muscle was homogenized at top speed for 10 s on ice using a Polytron

homogenizer (IKA Works, Inc., Wilmington, NC, USA). Five hundred milliliters of precooled buffer was used to homogenize the tissue. The buffer contained 20 mM of Tris-HCl with pH value equal to 7.4 and at initial temperature equal to 4 °C as well as 2% SDS, 5 mM EGTA, 5 mM EDTA, 1 mM DTT, 100 mM NaF, 2 mM sodium vanadate, 10 mg/ml pepstatin, 0.5 mM phenylmethylsulfonyl fluoride (PMSF), and 10 mg/ml leupeptin [25,26]. Each of the muscle homogenates was mixed with an equal volume of 2X SDS-PAGE loading buffer containing 0.5 M TrisHCl (pH 6.8), 2% (v/v) 2-mercaptoethanol, 20 vol% glycerol, 4.4% (w/v) SDS, and 0.01% bromophenol blue (boiled for 5 min prior to electrophoresis).

The gels were cast using a BioRad mini-gel system (Richmond, CA, USA) that was also used to perform the SDS-PAGE electrophoresis. Gradient gels of 5–20% were used to separate the proteins. When the electrophoresis was complete, proteins separated on the gels were moved to nitrocellulose membranes using buffer that contained 20 mM Tris-base, 0.1% SDS, 20% methanol, and 192 mM glycine. Next, the membranes were subjected to incubation in a blocking solution composed of 5% zero fat dry milk in TBS/T (150 mM NaCl, 50 mM Tris-HCl (pH 7.6), and 0.1% Tween-20 for 1 h. Then, these membranes were subsequently incubated overnight for the Western blotting using one of two types of antibodies: monoclonal anti- $\beta$ -actin antibody (Sigma-Aldrich, St Louis, MA, USA) or a primary antibody, anti-phospho-AMPK $\alpha$  (Thr 172, obtained from Cell Signaling Technology, Danvers, MA, USA). The membranes were washed 3 times (5 min each) using 20 mL of TBS/T following incubation with the primary antibody. The next step involved the incubation of the membranes with horseradish peroxidase-conjugated secondary antibodies that had been diluted 5-fold. These membranes were agitated gently for 1 h in TBS/T, followed by washing 3 times (10 min each time). Enhanced chemiluminescence (ECL) Western blotting reagent (from Amersham Bioscience) was used to visualize the membranes by exposing them to Biomax MR film (Kodak, Rochester, NY, USA). An Imager Scanner II and Image Quant TL software were used to quantify density of the bands [27]. Samples obtained after all these treatments were analyzed on a single gel to decrease variation between the blots. Reference band density was used to normalize band densities from different blots. In addition, the density of the  $\beta$ -actin band was also used to normalize the band densities.

### 2.7. Real-time PCR Analysis

Real-time reverse transcription (RT)-PCR was used to quantify expression levels of the genes selected for the analysis (see Table 1 for primer sequence) [28]. Briefly, TRIzol reagent (Invitrogen Corp., USA) was used to extract total RNA from the LD based on the method recommended by a manufacturer. RT was performed using Oligo(dT) random 6-mer primers from a Prime Script RT Master Mix kit (TaKaRa, Dalian, China) according to the manufacturer's instructions. A SYBR Premix Ex Taq kit (TaKaRa, Dalian, China) was used to perform quantitative PCR on a CFX96 Real-Time PCR detection system (BioRad). All of the experiments analyzed each RNA sample in triplicate. In addition, each experiment involved a negative control that lacked a cDNA template.  $\Delta\Delta C_t$  method (based on the report of Livak and Schmittgen, 2001) was implemented to obtain relative expression levels of the target mRNAs.

**Table 1.** Primer sequences and parameter used for real-time quantitative PCR [29].

Gene Symbol	No.	Gene Bank	Primers 5'-3'	GC%	Tm	Amplification Length/bp
PRKAA1	BA040395	NM0011098022	F-CACACATGAATGCAAAGATAGCTGA	40.0	63.5	109
			R-ATTACTTCTGGTGCAGCATAGTTGG	44.0	62.8	
PRKAA2	BA073991	NM0012056051	F-GAAGATCGGCCACTACGTGCT	57.1	63.8	93
			R-ACTTTATGGCCTGTCAATTGATGCT	40.0	64.1	

(Graphpad Prism; La Jolla, CA, USA). Significance was set at  $p < 0.05$ .

$$\text{Fold Change} = 2^{-\Delta\Delta\text{CT}}$$

$$\Delta\Delta\text{CT} = (\text{CT.Target gene} - \text{CT.}\beta - \text{actin})_x - (\text{CT.Target gene} - \text{CT.}\beta - \text{actin})_{\text{control}}$$

### 2.8. Data Processing and Statistical Analyses

A one-way analysis of variance (ANOVA) was implemented to obtain statistical significance for the differences using IBM SPSS 19.0 Software (SPSS, Inc., Chicago, IL, USA). Duncan's multiple range test was used for significance determination among the groups. At  $p < 0.05$ , results were considered statistically significant. The dynamics and graph plotting were conducted using Origin 8.0 software. Each experiment was repeated at least three times.

## 3. Results

### 3.1. pH Value Determination

AICAR injection in the postmortem LD muscle increased the decline in pH, while STO-609 decreased the same (Figure 1). The muscle pH was similar across all groups at 0 h postmortem and increased sharply in the control samples after 12 h ( $p < 0.05$ ) compared to that of AICAR-treated muscle, but was lower than the STO-609-treated muscle. At 24 h postmortem, the pH of the AICAR-injected yak muscle remained less than 6, indicating a high glycolytic rate (Figure 1).

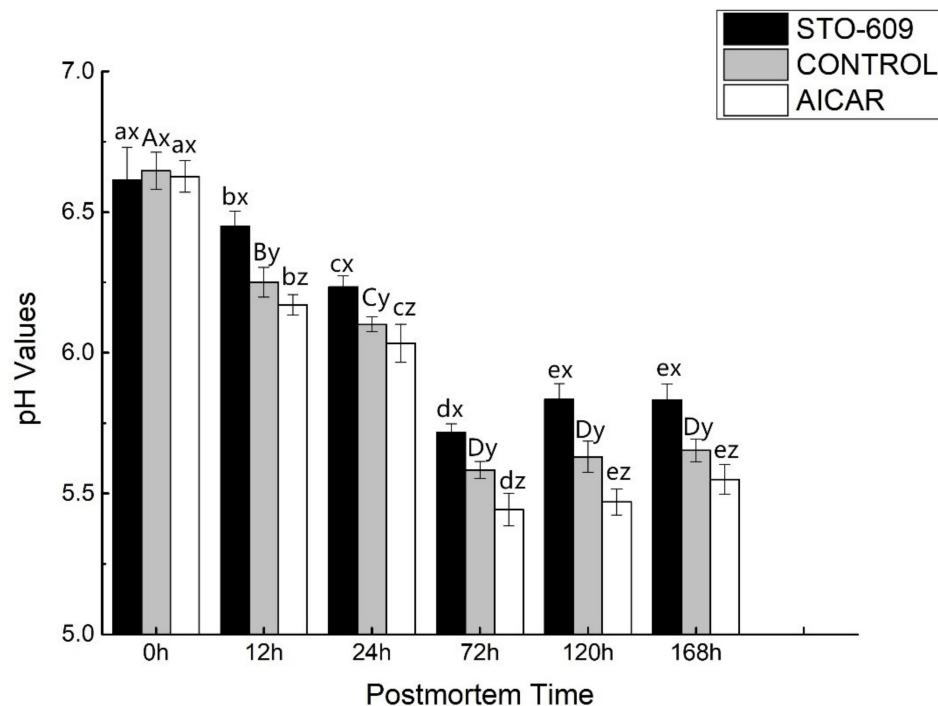


**Figure 1.** pH values of postmortem yak *longissimus dorsal* muscle. One-way ANOVA was used for statistical analyses between the control group and two treatment groups at 0 h to 168 h (three repetitions for each yak and 10 yaks from each group) (x, y, z  $p < 0.05$ ). Duncan's New Multiple-range test was used for the differences between the control group and two treatment groups at 0 h to 168 h. At 0 h, the lowercase letters represent the difference of the treatment group, and the capital letters represent stands the difference of the control group over time ( $p < 0.05$ ). Error bars indicate the standard errors of the mean.

### 3.2. Lactic Acid Concentration

Increased glycolysis in the AICAR-injected skeletal muscle was confirmed by the higher lactic acid accumulation rate (Figure 2). In addition to lowering the pH, STO-609 also reduced postmortem lactate accumulation in the LD muscle (Figure 2). The baseline muscle lactic acid concentration was similar between the differentially treated groups. From 0 to 72 h postmortem, the lactic acid concentration increased to  $126.56 \pm 5.89$  mg/g muscle in the control group compared to only  $96.32 \pm 3.19$  mg/g muscle in the STO-609-treated group, indicating that STO-609 inhibited lactic acid production in postmortem muscle at the initial stage. During the same time window, lactic acid concentration in the AICAR-treated muscle increased by  $132.51 \pm 6.32$  mg/g, indicating that AICAR activates lactic acid production in the initial stage of postmortem muscle. These findings suggested involvement of a novel glucose transporter.

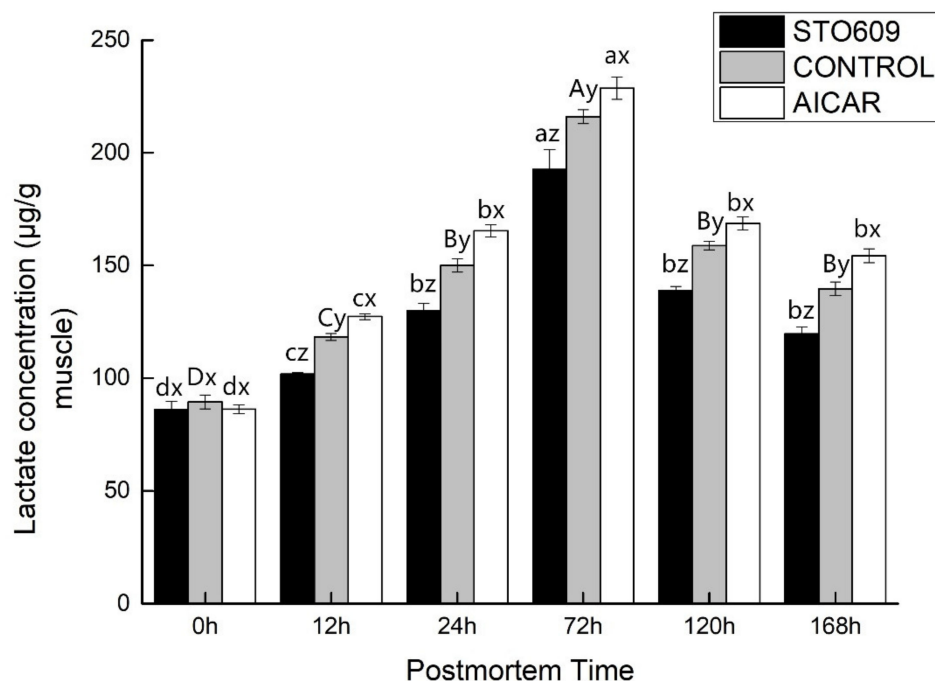


Figure 2. Lactic acid in postmortem yak *longissimus dorsal* muscle.

### 3.3. ATP, ADP, AMP, and IMP Activities

The nucleotide concentration in the yak LD muscle was measured in this study. After the 0 h control, there were no significant differences in nucleotide concentration observed between the control and treatment groups (Table 2). However, AICAR injection increased the ATP levels of the skeletal muscle while decreasing the concentrations of AMP and IMP ( $p < 0.05$ ). This result could be due to the inhibition of glycolysis in the LD muscle by the AICAR injection (Table 2). The AICAR injection inhibited glycolysis in the postmortem muscle (Figures 2 and 3). As a result of this inhibition, less ATP was produced, and the ATP concentration increased within 12 hours following death (Table 2). The IMP in the muscles of the yaks was also significantly higher than the AMP following the slaughter of the animals, and these results are consistent with those of previous studies (Shen et al., 2007; Shen et al., 2006). This result reiterated an observation that postmortem skeletal muscle delamination results in the rapid conversion of AMP to IMP. In the 0 h control, the nucleotide concentrations between the three groups did not differ significantly (Table 2). However, STO-609 injection resulted in a decrease in the concentration of ATP in the skeletal muscle and an increase in AMP and IMP at 12 h postmortem ( $p < 0.05$ ). This result can be explained by the inhibition of glycolysis due to the injection of STO-609 into the yak LD muscle. STO-609 injection inhibited glycolysis of the postmortem muscles (Figures 1 and 2), resulting in lower amounts of ATP production and therefore, a decrease in ATP concentration

at 12 h (Table 2). In addition, the data showed that the levels of IMP greatly exceeded those of AMP in the postmortem yak muscles, buttressing the results of previous reports (e.g., Shen et al., 2007; Shen, Thompson et al., 2006). This finding reiterates the importance of AMP. The skeletal postmortem muscle undergoes rapid conversion to IMP by the process of deamination. A decrease in the glycolysis of yak LD muscle injected with STO-609 indicates that the glycolysis of the skeletal postmortem muscle is partially regulated by AMPK.

**Table 2.** Nucleotide concentrations in postmortem yak *longissimus dorsal* muscle.

Time	0 h	12 h	24 h	72 h	120 h	168 h
ATP contents (lmol/g muscle)						
STO-609	3.00 ± 0.083 <sup>ax</sup>	1.69 ± 0.032 <sup>bx</sup>	1.58 ± 0.032 <sup>cx</sup>	0.11 ± 0.033 <sup>ex</sup>	0.32 ± 0.087 <sup>dx</sup>	0.45 ± 0.034 <sup>dx</sup>
Control	3.01 ± 0.093 <sup>Ax</sup>	1.95 ± 0.062 <sup>By</sup>	1.84 ± 0.053 <sup>Cy</sup>	0.22 ± 0.056 <sup>Ey</sup>	0.51 ± 0.067 <sup>Dy</sup>	0.61 ± 0.055 <sup>dy</sup>
AICAR	3.01 ± 0.041 <sup>ax</sup>	2.26 ± 0.055 <sup>bz</sup>	2.18 ± 0.051 <sup>cz</sup>	0.57 ± 0.036 <sup>ez</sup>	0.73 ± 0.025 <sup>dz</sup>	0.81 ± 0.020 <sup>dz</sup>
ADP contents (lmol/g muscle)						
STO-609	3.91 ± 0.031 <sup>ax</sup>	1.72 ± 0.046 <sup>bx</sup>	0.035 ± 0.043 <sup>ex</sup>	0.041 ± 0.072 <sup>dx</sup>	0.57 ± 0.042 <sup>cx</sup>	0.58 ± 0.021 <sup>cx</sup>
Control	3.99 ± 0.026 <sup>Ax</sup>	1.91 ± 0.073 <sup>By</sup>	0.54 ± 0.070 <sup>Dy</sup>	0.77 ± 0.112 <sup>Cy</sup>	0.72 ± 0.087 <sup>Cy</sup>	0.80 ± 0.025 <sup>Cy</sup>
AICAR	4.03 ± 0.042 <sup>az</sup>	2.11 ± 0.045 <sup>bz</sup>	0.89 ± 0.036 <sup>dz</sup>	1.02 ± 0.078 <sup>cz</sup>	1.05 ± 0.031 <sup>cz</sup>	1.06 ± 0.055 <sup>cz</sup>
AMP contents (lmol/g muscle)						
STO-609	0.24 ± 0.011 <sup>ax</sup>	0.09 ± 0.032 <sup>cx</sup>	0.12 ± 0.028 <sup>bx</sup>	0.065 ± 0.002 <sup>dx</sup>	0.058 ± 0.005 <sup>ex</sup>	0.031 ± 0.015 <sup>fx</sup>
Control	0.25 ± 0.015 <sup>Ax</sup>	0.14 ± 0.011 <sup>Cy</sup>	0.18 ± 0.009 <sup>By</sup>	0.11 ± 0.006 <sup>Dy</sup>	0.087 ± 0.005 <sup>Ey</sup>	0.077 ± 0.007 <sup>Fy</sup>
AICAR	0.25 ± 0.004 <sup>ax</sup>	0.20 ± 0.010 <sup>cz</sup>	0.25 ± 0.008 <sup>bz</sup>	0.17 ± 0.003 <sup>dz</sup>	0.104 ± 0.007 <sup>ez</sup>	0.100 ± 0.003 <sup>gz</sup>
IMP contents (lmol/g muscle)						
STO-609	1.32 ± 0.021 <sup>fx</sup>	1.96 ± 0.098 <sup>ex</sup>	2.43 ± 0.121 <sup>dx</sup>	5.42 ± 0.024 <sup>ax</sup>	3.72 ± 0.021 <sup>cx</sup>	4.15 ± 0.045 <sup>bx</sup>
Control	1.34 ± 0.018 <sup>Fy</sup>	2.28 ± 0.110 <sup>Ey</sup>	2.67 ± 0.180 <sup>Dy</sup>	5.74 ± 0.010 <sup>Ay</sup>	4.05 ± 0.015 <sup>Cy</sup>	4.38 ± 0.036 <sup>By</sup>
AICAR	1.34 ± 0.122 <sup>gz</sup>	2.57 ± 0.105 <sup>ez</sup>	2.84 ± 0.115 <sup>dz</sup>	5.96 ± 0.012 <sup>az</sup>	4.31 ± 0.002 <sup>cz</sup>	4.56 ± 0.101 <sup>bz</sup>

One-way ANOVA was used for statistical analyses between the control group and two treatment groups at 0 h to 168 h ( $x, y, z, p < 0.05$ ). Duncan's New Multiple-range test was used for the differences between the control group and two treatment groups at 0 h to 168 h. At 0 h, the lowercase letters represent the difference of the treatment group ( $a, b, c, d, e, f, p < 0.05$ ), and the capital letters represent the difference of the control group over time ( $A, B, C, D, E, F, p < 0.05$ ). Error bars indicate the standard errors of the mean.

### 3.4. AMPK Activity

Figure 3 shows the activity of AMPK in the postmortem yak LD. At the 0 h postmortem control, the activities of AMPK were  $1.56 \pm 0.06$ ,  $1.19 \pm 0.13$ , and  $1.00 \pm 0.07$  nmol of ATP per min per gram of the muscle mass for the AICAR and STO-609 treatments and the control, respectively. Representative AMPK activity is shown in Figure 3. The activation of AMPK was more rapid in the AICAR group and reached its maximal level at 12 h postmortem (Figure 3). At this same time, AMPK activity in the AICAR treatment exceeded those of the control and the STO-609 groups at  $2.39 \pm 0.19$  nmol of ATP per min per gram of the muscle mass. These results indicated that a more rapid activation of AMPK, and therefore higher activity, explained the faster decline in pH values and the higher rate of glycolysis during the early stage postmortem muscle of the yak.

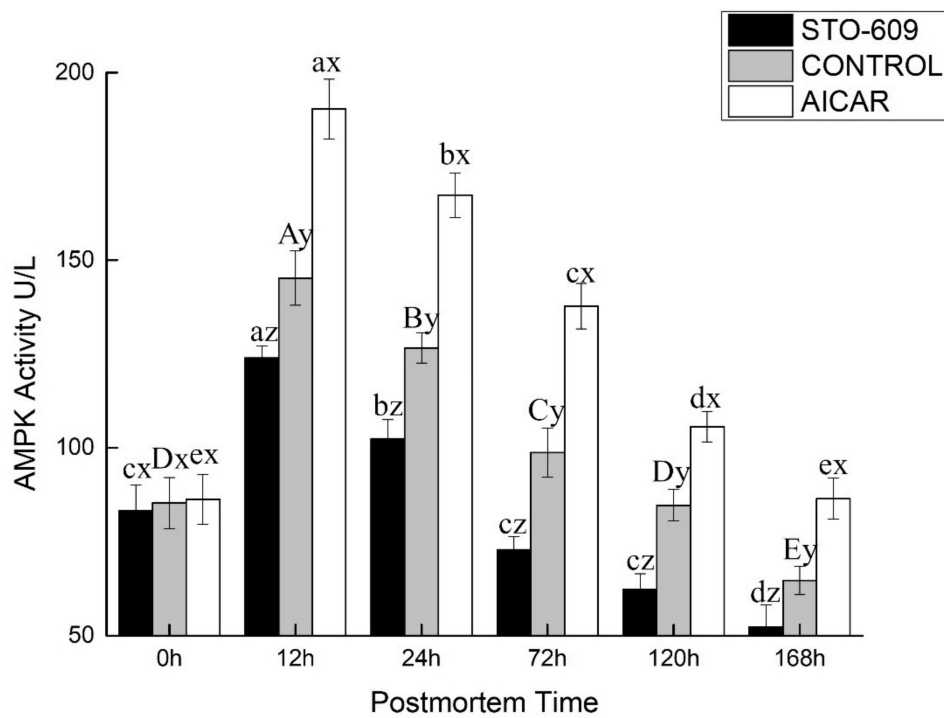
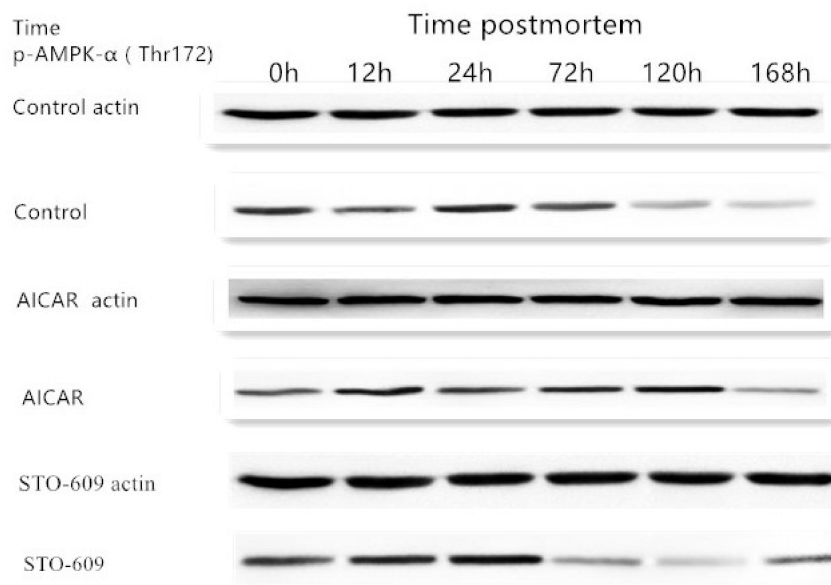


**Figure 3.** AMPK Activity of postmortem yak *longissimus dorsal* muscle. At a specific postmortem time, it indicates significant difference at  $p < 0.05$ .

### 3.5. Immunoprecipitation of AMPK

Figure 4A shows effects of intraperitoneal injection of AICAR and STO-609 on AMPK phosphorylation (Thr 172) in postmortem yak longissimus dorsi muscle. Representative immunoblots of AMPK phosphorylation and b-actin, and the relative band density of phospho-AMPK after normalizing to b-actin, are shown. Figure 4B shows densitometric analysis of AMPK expression of bovine muscle during postmortem aging.



(A)

**Figure 4.** Cont.



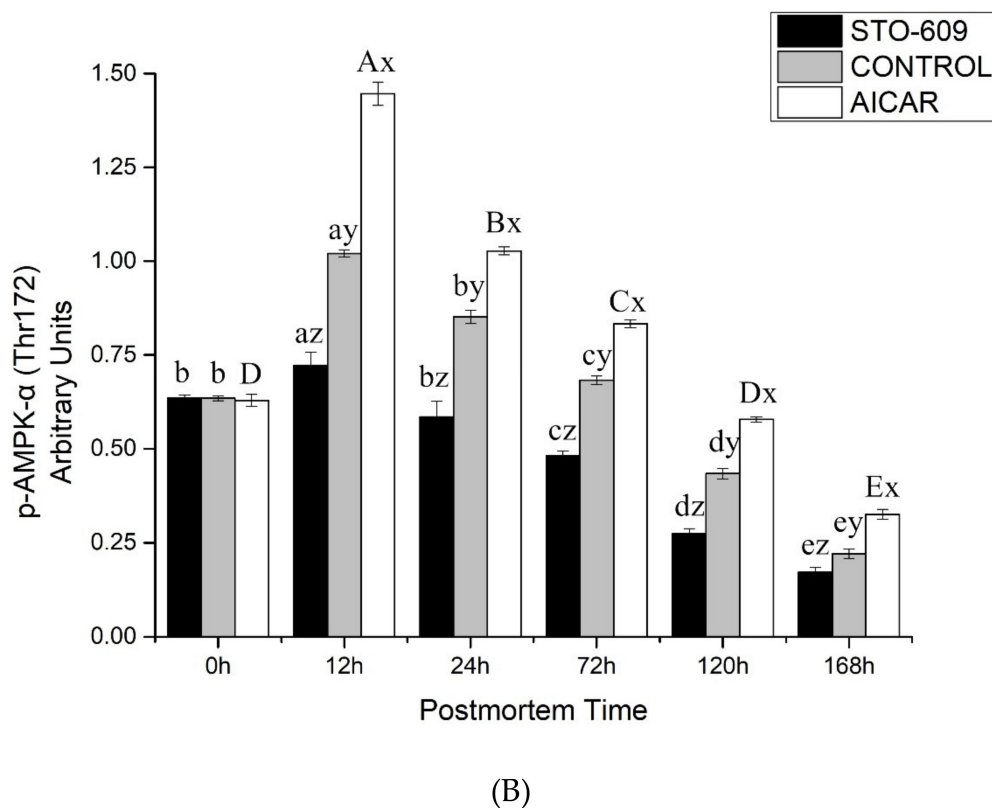
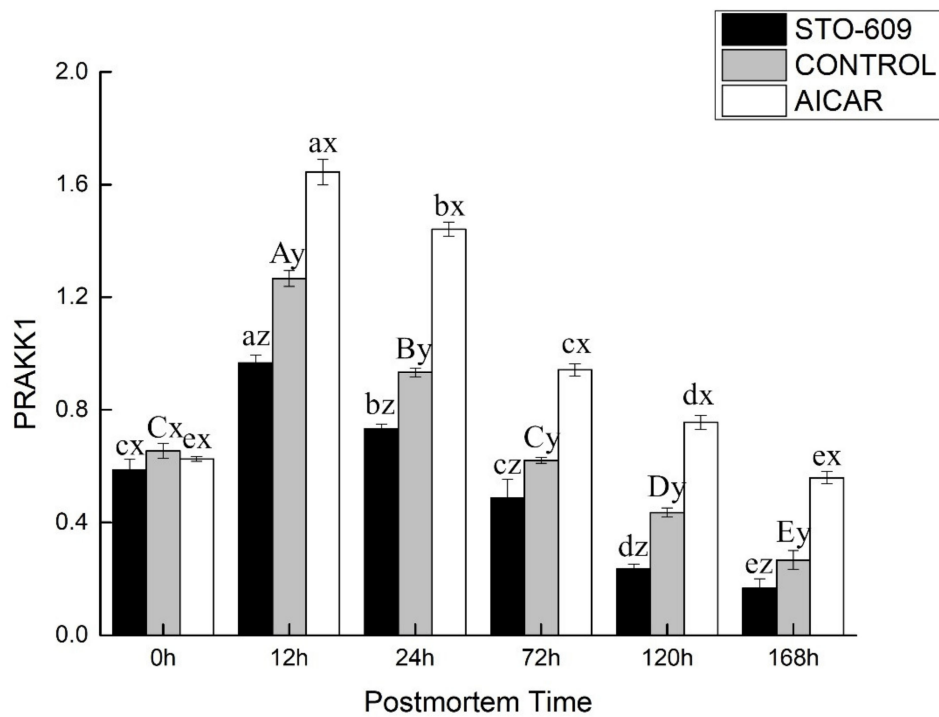
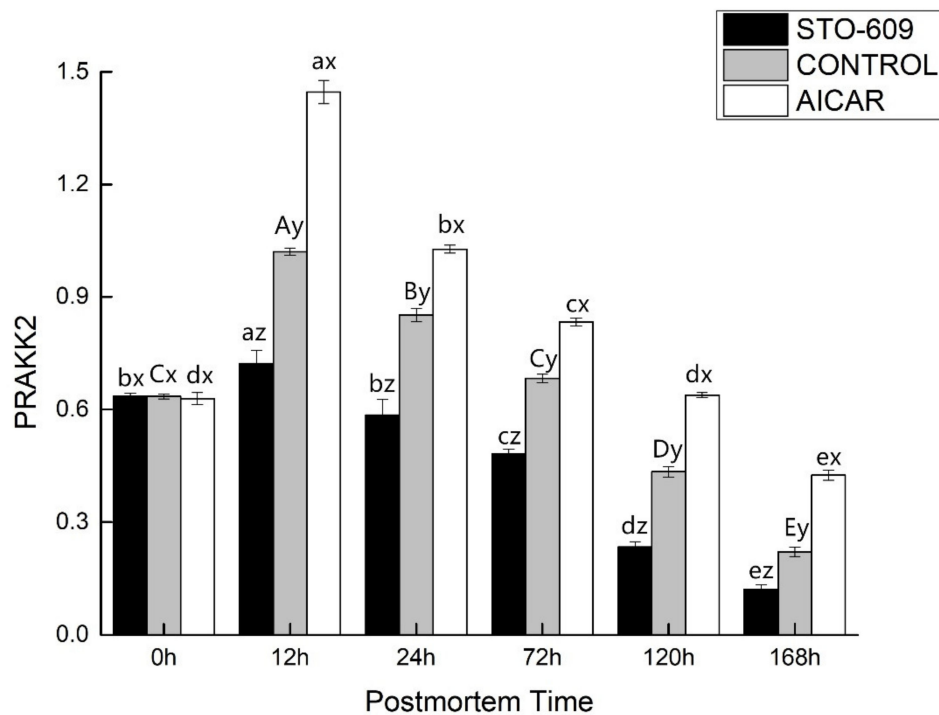


**Figure 4.** (A) Effects of intraperitoneal injection of AICAR and STO-609 on AMPK phosphorylation (Thr 172) in postmortem yak longissimus dorsi muscle. Representative immunoblots of AMPK phosphorylation and b-actin, and the relative band density of phospho-AMPK after normalizing to b-actin, are shown. (B) Densitometric analysis of AMPK expression of bovine muscle during postmortem aging.

The main goal of this work was to study the influence of STO-609 and AICAR on postmortem glycolysis and AMPK activity. STO-609 functions as a specific competitive inhibitor of AMPK and has been well studied [28,30]. A representative immunoblot shown in Figure 5 demonstrates AMPK phosphorylation. As expected, the postmortem muscle yak LD AMPK phosphorylation was reduced following the injection of STO-609 (Figure 5). The activities of AMPK were higher in the skeletal muscle after death following STO-609 without sputum injection, and the greatest amount of activity was detected at 12 h postmortem. However, in the samples treated with STO-609, no significant change in the levels of AMPK activity as a result of the aging time was observed (Figure 4). After 0–12 h postmortem, the level of phosphorylation of AMPK in the control group increased by  $0.39 \pm 0.02$  arbitrary units, and this was greater than the  $0.20 \pm 0.01$  arbitrary units in the LD muscle after the STO-609 injection ( $p < 0.05$ ). In the muscles of the yak injected with STO-609, AMPK phosphorylation was decreased because the subunit Thr 172 delayed the decrease in AMPK activity. However, from the 0 to 12 h samples postmortem, the phosphorylation of AMPK increased by  $0.39 \pm 0.02$  arbitrary AICAR units. This increase was higher than the  $0.20 \pm 0.01$  arbitrary units in the postmortem LD yak muscle without injection ( $p < 0.05$ ). Increased AMPK phosphorylation of the subunit at Thr 172 indicates higher AMPK activity in yak postmortem muscle subjected to AICAR injection.



(A)



(B)

**Figure 5.** Effect of AICAR and STO-609 on AMPK $\alpha$ 1(A), AMPK $\alpha$ 2 (B) mRNA. The samples were treated with or without AICAR (10 mM) and STO-609 (10 mM) for the time as indicated above, and total RNA was subjected to real-time RT-PCR as described in Materials and Methods. The results are expressed as a relative value compared to the untreated sample as 100%. All data were represented as means  $\pm$  SEM of three independent experiments.  $p < 0.05$ , compared with the untreated control.

### 3.6. Gene Expression of AMPK

Previous studies demonstrated that line injections of AICAR and STO-609 in yak could involve the hypothalamic AMPK system. To determine whether the AMPK system mediated the effect of AICAR, the gene expression of different AMPK subunit levels of gene expression was tested. The results indicated mRNA level increased in the yak hypothalamic  $\alpha 1$  subunit of AMPK after AICAR injection. The phosphorylation of AMPK is mediated by the cooperation of these different subunits, which was shown to correlate with AMPK activity. This study indicates that the AICAR injection caused different effects on the catalytic and regulatory AMPK subunits. The mRNA expression of the regulatory subunits  $\alpha 1$  and  $\alpha 2$  was stimulated by AMPK. These results suggest the increase in AMPK activity may be due to an independent mechanism that could be inhibited by STO-609. The fact that the regulatory subunits  $\beta$  and  $\gamma$  can only result in catalytic activity when they are in a complex with the  $\alpha$  subunits has strong implications for the role of the catalytic subunits in the activity of AMPK. It suggests that their availability is a key determinant of this activity. Although there is not enough data on AMPK's role in glucose metabolism regulation to make firm conclusions, our research provides the first analysis of the effect that an AMPK agonist has on glucose metabolism in yaks. These results confirm the promotion of glucose uptake in yak muscle by AICAR. In addition, the results suggest that this process may be due to the mediation of a novel glucose transporter. In total, these results provide confirmation that STO-609 acts as a potent AMPK inhibitor and causes a reduction of AMPK activity in postmortem yak muscles.

## 4. Discussion

The activation of AMPK during such stresses, accompanied by increases in cellular AMP, triggers changes in the rates of glucose transport, lipogenesis, sterol synthesis, and gluconeogenesis, which serve to both preserve the needed ATP and increase the rate of ATP generation. AMPK is a heterotrimer consisting of a catalytic subunit and two noncatalytic subunits,  $\beta$  and  $\gamma$ . Each subunit is a member of a larger isoform family consisting of two alpha subunits  $\alpha 1$  and  $\alpha 2$ , two beta subunits  $\beta 1$  and  $\beta 2$ , and three gamma subunits  $\gamma 1$ ,  $\gamma 2$ , and  $\gamma 3$ , all of which show varying tissues and subcellular expressions [31]. This study focused on how AICAR and STO-609 affected the AMPK pathway, which is related to energy metabolism in the yak LD muscle. Our results suggest that AICAR and STO-609 induce changes in parameters involved in energy metabolism. AMPK functions to regulate the metabolism of energy and substrates, primarily the metabolism of carbohydrates and the homeostasis of whole-body energy. AMPK acts as an energy sensor for the whole body to meet both body energy and cellular requirements by integrating different signaling pathways, while also activating energy-producing processes and inhibiting those processes that consume energy [32]. AMPK primarily promotes fatty acid and glucose catabolism, while preventing the synthesis of glycogen.

The involvement of AMPK in both lipid and glucose metabolism has been reported. Stress induced by nutrients or exercise increases the level of AMP at the cellular levels. This increase accelerates beta oxidation of fatty acids as well as glucose transport into skeletal muscles. In contrast, AMPK activation inhibits several gene transcriptions, apoptosis, and cholesterol and fatty acid syntheses. The injection of STO-609 reduces the decline in pH and the accumulation of lactic acid in postmortem murine LD muscle (Figures 1 and 2). In concert, the intraperitoneal injection of STO-609 into murine early-stage postmortem muscle tissue demonstrated the initial inhibition of the level of postmortem glycolysis due to the development of lower lactic acid concentrations and higher pH values in the tissue. The injection of AICAR increased the accumulation of lactic acid and the decline in pH values in the muscle of postmortem murine LD (Figures 1 and 2). In concert, the development of higher concentrations of lactic acid and lower pH values in the early stage yak postmortem muscle following AICAR injection indicated that the level of initial postmortem glycolysis increased due to the effects of AICAR. Implementation of a combination of STO-609 as a specific AMPK inhibitor and commonly used AICAR as an activator of AMPK in an array of cellular systems suggest that AMPK mediates

postmortem glycolysis reduction. Thus, this study confirms previous ones that indicate postmortem skeletal muscle glycolysis is AMPK regulated [16,33].

AMPK performs an important part in substrate and energy metabolism due to its regulation of signaling pathways. AMPK monitors the availability of nutrients as well as AMP/ATP and ADP/ATP ratios, which enables it to sense the status of cellular energy levels. AMPK also regulates events in the cell by both inhibiting reactions and activates consuming ATP (e.g., protein and fatty acid syntheses) as well as cellular processes generating ATP (e.g., fatty acid oxidation, glucose uptake, and glycolysis) [2].

Previous reports demonstrated that preslaughter stress quickened depletion of muscle ATP levels. This reduction in the status of energy therefore results in the early and rapid activation of AMPK in early postmortem stages, which makes it more likely that pork loin will develop into PSE meat [21,34]. The primary AMPK function is the regulation of the internal cellular energy balance (Hardie et al., 2003; Hardie et al., 1999; Winder and Hardie, 1999). ATP depletion results in the activation of AMPK, or to be more precise, an AMP/ATP ration increase [15,35]. AMPK is affected by the binding of AMP occurring at low intracellular energy levels and high concentrations of AMP. AMPK changes its conformation and becomes a more effective substrate for LKB1, which is also known as upstream AMPK kinase [7]. Additionally, LKB1 activates AMPK by phosphorylating it [36]. Activation of AMPK results in the switching on of fatty acid oxidation and glycolysis, which results in the production of greater amounts of ATP inside the cells [37]. Earlier research demonstrated that the halothane gene and the stress of the preslaughter process accelerated the depletion of muscle ATP levels. The reduction in the cellular energy status during the early postmortem state subsequently leads to the earlier and quicker activation of AMPK, which increases the risk of the development of PSE in pork loin [16,34].

Since STO-609 injections in murine LD muscle tissue result in decreased glycolysis, they have implications for the regulation of AMPK in this type of tissue. The results of these experiments in postmortem skeletal muscle suggest the partial regulation of glycolysis by AMPK. Previous studies suggest that glycolysis in ischemic cardiac muscle is increased by AMPK at two primary points: one is phosphor-fructose kinase 1 (PFK1), while the other is glycogen phosphorylase. The activation of AMPK can upregulate glycolysis due to its ability to activate and phosphorylate phosphorylase kinase. In turn, phosphorylated kinase can then phosphorylate and activate glycogen phosphorylase, which is an enzyme controlling glycogenolysis and catalyzing glycolysis substrate production [17–19]. In addition, activated AMPK is responsible for the phosphorylation and activation of phosphofructokinase-2 (PFK-2) [16]. In turn, activated PFK-2 catalyzes fructose-2,6-phosphate production. PRK-1 is the most important enzyme controlling the rate of glycolysis, and the enzyme is activated allosterically by fructose-2,6-phosphate.

In humans and mice, AICAR is commonly used as an AMPK activator; its role in AMPK activation in LD muscle was established by McFadden and Corl [38]. This role was confirmed in yak LD muscle during differentiation in this study. As expected, STO-609 injection decreased the phosphorylation of AMPK in LD muscle from postmortem yak, but AICAR had the opposite effect. AMPK could still be activated in postmortem yak skeletal muscle that had not been injected with STO-609, and the greatest amounts of activity were detected in the 12 h postmortem samples. However, the postmortem samples that had been injected with STO-609 did not exhibit any changes in the activity of AMPK activity over time. In addition, the postmortem yak samples that had been treated with STO-609 had lower levels of ACC phosphorylation at Thr 172. This result was consistent with the lower amounts of AMPK activity and also with the findings of previous research [33]. In concert, these findings confirm that STO-609 is a potent inhibitor of AMPK, which leads to lower levels of activity of AMPK in the postmortem skeletal yak muscle.

We implemented real-time RT-PCR to examine AMPK mRNA expression affected by AICAR. The purpose of this experiment was to identify the mechanisms by which AICAR induces the activation of the AMPK protein. Figure 5 shows that the expression of the mRNA of AMPK increased significantly at 12 h after treatment with AICAR. This figure also shows the dose-dependent manner in which

12 h treatments with STO-609 induced effects opposite to those of AICAR. Thus, suppression of AMPK mRNA expression was one of the mechanisms by which STO-609 induced the reduction of the AMPK protein. However, the mechanisms by which AICAR induces a high-level regulation of the AMPK gene via AMPK activation remain unclear. One possible mechanism by which AMPK could be transcriptionally regulated could involve the modification of transcription factors by their direct phosphorylation. In addition, it has been reported that AMPK decreases the amount of glucose by modifying its stability. These results raise the possibility that AMPK could directly target glucose and that its phosphorylation of glucose could increase the rate of degradation of this compound. Another way in which AMPK-induced transcriptional reduction could affect the metabolism of the tissue is through the phosphorylation of the cofactors that control the activity of transcription. For example, AMPK causes a reduction in the affinity of p300 for multiple nuclear receptors by phosphorylating it on Ser89. This reaction results in a decrease in the affinity of p300 for multiple nuclear receptors (e.g., thyroid hormone and peroxisome proliferator-activated receptors (PPAR)  $\alpha$  and  $\beta$ ). However, this study did not enable us to identify the transcription factors that were responsible for regulation increase in the gene expression of AMPK induced by AICAR. Therefore, additional research to identify the transcription factors and cis-elements that are involved in the response to AICAR is merited.

## 5. Conclusions

The changes in beef glycolysis, energy metabolism, AMPK activity and the expression of the AMPK gene (PRKKA1, PRKKA2) in Yushu yak during the postmortem period were measured. The results of this study demonstrate that the expression of the PRKAA1 and PRKAA2 genes and the AMPK activity were subject to AICAR activation and STO-609 inhibition. This suggests that the increased expression of the PRKAA1 and PRKAA2 genes will increase the activity of AMPK. After AMPK is activated, the direct phosphorylation glycolysis pathway increases the glycolysis activity, which promotes the glycolysis process and produces a large amount of lactic acid. This production results in the decrease of energy metabolism in postmortem animal muscles. Therefore, the activity of the yak AMPK increased under hypoxic adaptation, which accelerated glycolysis and metabolism and more effectively regulated energy production. It laid a foundation for the establishment of the theoretical system of energy metabolism in postmortem yak meat.

**Author Contributions:** Conceptualization, Y.Y.; methodology, Y.Y.; software, Y.Y.; validation, Y.Y. and Y.G.; formal analysis, L.H.; investigation, Y.Y. and R.S.; resources, R.S.; data curation, L.H.; writing—original draft preparation, Y.Y.; writing—review and editing, Y.Y. and Q.Y.; visualization, L.H.; supervision, L.H. and Q.Y.; project administration, L.H.; funding acquisition, L.H. and Q.Y. All authors have read and agreed to the published version of the manuscript.

**Funding:** This work was supported by the National Beef Cattle Industrial Technology System (CARS-37), National Natural Science Foundation of China (Grant Nos: 31760482).

**Acknowledgments:** We thank colleagues in the laboratory and our collaborators for their useful suggestions.

**Conflicts of Interest:** The authors have declared no conflict of interest.

## References

1. Zuo, H.X.; Han, L.; Yu, Q. Proteomics and bioinformatics analyses of differentially expressed proteins in yak and beef cattle muscle. *Trans. Chin. Soc. Agric. Mach.* **2017**, *48*, 313–320.
2. Hardie, D.G.; Scott, J.W.; Pan, D.A.; Hudson, E.R. Management of cellular energy by the AMP-activated protein kinase system. *FEBS Lett.* **2003**, *546*, 113–120. [[CrossRef](#)]
3. Hardie, D.G.; Ross, F.A.; Hawley, S.A. AMPK: A nutrient and energy sensor that maintains energy homeostasis. *Nat. Rev. Mol. Cell Biol.* **2012**, *13*, 251–262. [[CrossRef](#)] [[PubMed](#)]
4. Ding, X.Z.; Liang, C.N.; Guo, X.; Wu, X.Y.; Wang, H.B.; Johnson, K.A.; Yan, P. Physiological insight into the high-altitude adaptations in domesticated yaks (*Bos grunniens*) along the Qinghai-Tibetan Plateau altitudinal gradient. *Livest. Sci.* **2014**, *162*, 233–239. [[CrossRef](#)]

5. Chen, Z.P.; Stephens, T.J.; Murthy, S.; Canny, B.J.; Hargreaves, M.; Witters, L.A.; Kemp, B.E.; McConell, G.K. Effect of exercise intensity on skeletal muscle AMPK signaling in humans. *Diabetes* **2003**, *52*, 2205–2212. [[CrossRef](#)]
6. Wojtaszewski, J.F.; Nielsen, P.; Hansen, B.F.; Richter, E.A.; Kiens, B. Isoform specific and exercise intensity-dependent activation of 5'-AMP-activated protein kinase in human skeletal muscle. *J. Physiol.* **2000**, *528*, 221–226. [[CrossRef](#)]
7. Musi, N.; Hayashi, T.; Fujii, N.; Hirshman, M.F.; Witters, L.A.; Goodyear, L.J. AMP-activated protein kinase activity and glucose uptake in rat skeletal muscle. *Am. J. Physiol. Endocrinol. Metab.* **2001**, *280*, E677–E684. [[CrossRef](#)]
8. Park, S.H.; Gammon, S.R.; Knippers, J.D.; Paulsen, S.R.; Rubink, D.S.; Winder, W.W. Phosphorylation activity relationships of AMPK and acetyl-CoA carboxylase in muscle. *J. Appl. Physiol.* **2002**, *92*, 2475–2482. [[CrossRef](#)]
9. Hardie, D.G. AMP-activated protein kinase: The guardian of cardiac energy status. *J. Clin. Investig.* **2004**, *114*, 465–468. [[CrossRef](#)]
10. Carling, D. The AMP-activated protein kinase cascade—A unifying system for energy control. *Trends Biochem. Sci.* **2004**, *29*, 18–24. [[CrossRef](#)]
11. Winder, W.W. Energy-sensing and signaling by AMP-activated protein kinase in skeletal muscle. *J. Appl. Physiol.* **2001**, *91*, 1017–1028. [[CrossRef](#)] [[PubMed](#)]
12. Hardie, D.G.; Carling, D. The AMP-activated protein kinase—fuel gauge of the mammalian cell? *Eur. J. Biochem.* **1997**, *246*, 259–273. [[CrossRef](#)] [[PubMed](#)]
13. Minokoshi, Y.; Alquier, T.; Furukawa, N.; Kim, Y.B.; Lee, A.; Xue, B.; Mu, J.; Fofelle, F.; Ferré, P.; Birnbaum, M.J.; et al. AMP-kinase regulates food intake by responding to hormonal and nutrient signals in the hypothalamus. *Nature* **2004**, *428*, 569–574. [[CrossRef](#)] [[PubMed](#)]
14. Hardie, D.G.; Salt, I.P.; Hawley, S.A.; Davies, S.P. AMP-activated protein kinase: An ultrasensitive system for monitoring cellular energy charge. *Biochem. J.* **1999**, *338*, 717–722. [[CrossRef](#)]
15. Corton, J.M.; Gillespie, J.G.; Hardie, D.G. Role of the AMP-activated protein kinase in the cellular stress response. *Curr. Biol.* **1994**, *4*, 315–324. [[CrossRef](#)]
16. Shen, Q.W.; Means, W.J.; Underwood, K.R.; Thompson, S.A.; Zhu, M.J.; McCormick, R.J.; Ford, S.P.; Ellis, M.; Du, M. Early post-mortem AMP-activated protein kinase (AMPK) activation leads to phosphofructokinase-2 and -1 (PFK-2 and PFK-1) phosphorylation and the development of pale, soft, and exudative (PSE) conditions in porcine longissimus muscle. *J. Agric. Food Chem.* **2006**, *54*, 5583–5589. [[CrossRef](#)]
17. Fan, X.; Ding, Y.; Brown, S.; Zhou, L.; Shaw, M.; Vella, M.C.; Cheng, H.; McNay, E.C.; Sherwin, R.S.; McCrimmon, R.J. Hypothalamic AMP-activated protein kinase activation with AICAR amplifies counterregulatory responses to hypoglycemia in a rodent model of type 1 diabetes. *Am. J. Physiol. Regul. Integr. Comp. Physiol.* **2009**, *296*, R1702–R1708. [[CrossRef](#)]
18. Vincent, M.F.; Erion, M.D.; Gruber, H.E.; Van den Berghe, G. Hypoglycaemic effect of AICA riboside in mice. *Diabetologia* **1996**, *39*, 1148–1155. [[CrossRef](#)] [[PubMed](#)]
19. Kim, E.K.; Miller, I.; Aja, S.; Landree, L.E.; Pinn, M.; McFadden, J.; Kuhajda, F.P.; Moran, T.H.; Ronnett, G.V. C75, a fatty acid synthase inhibitor, reduces food intake via hypothalamic AMP-activated protein kinase. *J. Biol. Chem.* **2004**, *279*, 19970–19976. [[CrossRef](#)]
20. Fernandez, X.; Neyraud, E.; Astruc, T.; Sante, V. Effects of halothane genotype and pre-slaughter treatment on pig meat quality. Part 1. Post-mortem metabolism, meat quality indicators and sensory traits of m. Longissimus Lumborum. *Meat Sci.* **2002**, *62*, 429–437. [[CrossRef](#)]
21. Shen, Q.W.; Means, W.J.; Thompson, S.A.; Underwood, K.R.; Zhu, M.J.; McCormick, R.J.; Ford, S.P.; Du, M. Pre-slaughter transport, AMP-activated protein kinase, glycolysis, and quality of pork loin. *Meat Sci.* **2006**, *74*, 388–395. [[CrossRef](#)] [[PubMed](#)]
22. Hou, Y.; Yao, K.; Wang, L.; Ding, B.; Fu, D.; Wu, G. Effects of alpha-ketoglutarate on energy status in the intestinal mucosa of weaned piglets chronically challenged with lipopolysaccharide. *Br. J. Nutr.* **2011**, *106*, 357–363. [[CrossRef](#)] [[PubMed](#)]
23. Shen, Q.W.; Jones, C.S.; Kalchayanand, N.; Zhu, M.J.; Du, M. Effect of dietary alpha-lipoic acid on growth, body composition, muscle pH, and AMP-activated protein kinase phosphorylation in mice. *J. Anim. Sci.* **2005**, *83*, 2611–2617. [[CrossRef](#)]

24. Veiseth, E.; Shackelford, S.D.; Wheeler, T.L.; Koohmaraie, M. Technical note: Comparison of myofibril fragmentation index from fresh and frozen pork and lamb longissimus. *J. Anim. Sci.* **2001**, *79*, 904–906. [[CrossRef](#)] [[PubMed](#)]
25. Raser, K.J.; Posner, A.; Wang, K.K.W. Casein zymography: A method to study  $\mu$ -calpain, m-calpain, and their inhibitory agents. *Arch. Biochem. Biophys.* **1995**, *319*, 211–216. [[CrossRef](#)] [[PubMed](#)]
26. Shen, Q.W.; Du, M. Effects of dietary alpha-lipoic acid on glycolysis of postmortem muscle. *Meat Sci.* **2005**, *71*, 306–311. [[CrossRef](#)]
27. Brüggemann, M.; Raff, T.; Flohr, T.; Gökbüget, N.; Nakao, M.; Droese, J.; Lüschen, S.; Pott, C.; Ritgen, M.; Scheuring, U.; et al. Clinical significance of minimal residual disease quantification in adult patients with standard-risk acute lymphoblastic leukemia. *Blood* **2006**, *107*, 1116–1123. [[CrossRef](#)]
28. Kim, E.T.; Madhukar, A.; Ye, Z.; Campbell, J.C. High detectivity inas quantum dot infrared photodetectors. *Appl. Phys. Lett.* **2004**, *84*, 3277. [[CrossRef](#)]
29. Proszkowiec-Weglarz, M.; Richards, M.P.; Ramachandran, R.; McMurtry, J.P. Characterization of the AMP-activated protein kinase pathway in chickens. *Comp. Biochem. Physiol. B Biochem. Mol. Biol.* **2006**, *143*, 92–106.
30. Blattler, S.M.; Rencurel, F.; Kaufmann, M.R.; Meyer, U.A. In the regulation of cytochrome P450 genes, phenobarbital targets LKB1 for necessary activation of AMP-activated protein kinase. *Proc. Natl. Acad. Sci. USA* **2007**, *104*, 1045–1050. [[CrossRef](#)]
31. Hamilton, S.R.; O'Donnell, J.B., Jr.; Hammet, A.; Stapleton, D.; Habinowski, S.A.; Means, A.R.; Kemp, B.E.; Witters, L.A. Amp-activated protein kinase kinase: Detection with recombinant AMPK alpha1 subunit. *Biochem. Biophys. Res. Commun.* **2002**, *293*, 892–898. [[CrossRef](#)]
32. Copenhafer, T.L.; Richert, B.T.; Schinckel, A.P.; Grant, A.L.; Gerrard, D.E. Augmented postmortem glycolysis does not occur early postmortem in AMPK73-mutated porcine muscle of halothane positive pigs. *Meat Sci.* **2006**, *73*, 590–599. [[CrossRef](#)] [[PubMed](#)]
33. Shen, Q.W.; Du, M. Role of AMP-activated protein kinase in the glycolysis of postmortem muscle. *J. Sci. Food Agric.* **2005**, *85*, 2401–2406. [[CrossRef](#)]
34. Shen, Q.W.; Underwood, K.R.; Means, W.J.; McCormick, R.J.; Du, M. The halothane gene, energy metabolism, adenosine monophosphate-activated protein kinase, and glycolysis in postmortem pig longissimus dorsi muscle. *J. Anim. Sci.* **2007**, *85*, 1054–1061. [[CrossRef](#)] [[PubMed](#)]
35. Birnbaum, M.J. Activating AMP-activated protein kinase without AMP. *Mol. Cells* **2005**, *19*, 289–290. [[CrossRef](#)] [[PubMed](#)]
36. Woods, A.; Johnstone, S.R.; Dickerson, K.; Leiper, F.C.; Fryer, L.G.; Neumann, D.; Schlattner, U.; Wallimann, T.; Carlson, M.; Carling, D. LKB1 is the upstream kinase in the AMP-activated protein kinase cascade. *Curr. Biol.* **2003**, *13*, 2004–2008. [[CrossRef](#)]
37. Carling, D.; Zammit, V.A.; Hardie, D.G. A common bicyclic protein-kinase cascade inactivates the regulatory enzymes of fatty-acid and cholesterol-biosynthesis. *FEBS Lett.* **1987**, *223*, 217–222. [[CrossRef](#)]
38. Mcfadden, J.W.; Corl, B.A. Activation of amp-activated protein kinase (ampk) inhibits fatty acid synthesis in bovine mammary epithelial cells. *Biochem. Biophys. Res. Commun.* **2009**, *390*, 388–393. [[CrossRef](#)]

